PERGAMON

International Journal of Solids and Structures 40 (2003) 4729–4748

INTERNATIONAL JOURNAL OF SOLIDS and STRUCTURES

www.elsevier.com/locate/ijsolstr

Nonlinear interactions in the planar dynamics of cable-stayed beam

Vincenzo Gattulli *, Marco Lepidi

Dipartimento di Ingegneria delle Strutture, delle Acque e del Terreno, Università di L'Aquila, P.le. E. Pontieri 2, 67040 Monteluco di Roio L'Aquila, Italy

Received 19 December 2002; received in revised form 2 May 2003

Abstract

An analytical model is proposed to study the nonlinear interactions between beam and cable dynamics in stayed-systems. The integro-differential problem, describing the in-plane motion of a simple cable-stayed beam, presents quadratic and cubic nonlinearities both in the cable equation and at the boundary conditions. Mainly studied are the effects of quadratic interactions, appearing at relatively low oscillation amplitude. To this end an analysis of the sensitivity of modal properties to parameter variations, in intervals of technical interest, has evidenced the occurrence of one-to-two and two-to-one internal resonances between global and local modes. The interactions between the resonant modes evidences two different sources of oscillation in cables, illustrated by simple 2dof discrete models.

In the one-to-two global–local resonance, a novel mechanism is analyzed, by which cable undergoes large periodic and chaotic oscillations due to an energy transfer from the low-global to high-local frequencies.

In two-to-one global–local resonance, the well-known parametric-induced cable oscillation in stayed-systems is correctly reinterpreted through the autoparametric resonance between a global and a local mode. Increasing the load the saturation of the global oscillations evidences the energy transfer from high-global to low-local frequencies, producing large cable oscillations. In both cases, the effects of detuning from internal and external resonance are presented.

Keywords: Cables; Cable-stayed beam; Galerkin; Sensitivity; Dynamic interaction; Nonlinear oscillations; Energy transfer; Autoparametric resonance

1. Introduction

In the past decade, an increasing interest has been devoted to cable-supported structures, mostly for their inherent mechanical effectiveness (Barsotti et al., 2001), but enhanced by valuable esthetic outcomes, as is appreciable in the recent construction of stayed bridges, guyed towers and suspended roofs.

* Corresponding author. Tel.: +39-0862-434511; fax: +39-0862-434548.
E-mail address: gattulli@ing.univaq.it (V. Gattulli).
URL: http://www.ing.univaq.it/webdisat/

0020-7683/03/$ - see front matter © 2003 Elsevier Ltd. All rights reserved.
doi:10.1016/S0020-7683(03)00266-X

However, these good qualities are often accompanied by undesired vibrations in both the main system and the cables due to the structural lightness, flexibility and inherent low damping characteristics. Numerous investigations have been conducted on overall dynamic behavior under environmental loading (Nazmy and Abdel-Ghaffar, 1990; Abdel-Ghaffar and Khalifa, 1991), on structural identification and on-line health monitoring (Casas, 1995; Gentile and Martinez Y Cabrera, 1997), and more recently on design of passive and active dissipation strategies (Warnitchai et al., 1993; Achkire and Preumont, 1996; Gattulli and Paolone, 1997; Magaña and Rodellar, 1998).

Nevertheless, understanding the dynamic interactions between the cables and the main structural components remains a crucial issue.

Refined finite element models for cable-stayed bridge dynamics have been used by Abdel-Ghaffar and his co-authors to demonstrate the importance of nonlinear dynamical analysis (Nazmy and Abdel-Ghaffar, 1990) and linear cable–beam interactions (Abdel-Ghaffar and Khalifa, 1991; Au et al., 2001). Starting from the observation that only global behavior is modeled in common dynamic analysis (where the cables are treated as equivalent tendon elements), Fujino and his co-authors, (Warnitchai et al., 1993, 1995) have enriched the dynamical description through an opportune treatment of local cable motion. In particular, they have proposed to investigate cable–beam interactions by means of a Ritz-type analytical model based on test functions representative of global and local modes and through an experimental set-up of a cable-stayed beam. Under their analytical model, global motions are described by cantilever eigenfunctions in the beam domain and quasi-static functions in the cable domain, while local motions are described by Irvine cable eigenfunctions. At the same time, in their experiments they have observed a so-called *modal distortion* indicating that linear coupling between the beam and the cable modifies the assumed cantilever modal shapes in a non-negligible way. Under the assumption of their model, they have also observed the phenomenon of autoparametric excitation due to a two-to-one resonance between the planar global and local modes and have analyzed its interactions with the out-of-plane local mode (Fujino et al., 1993).

At this stage, the main recognized sources of vibrations in cable-stayed systems are the induced direct and parametric boundary cable excitations by beam motion (Perkins, 1992; Fujino et al., 1993; Lilien and Pinto da Costa, 1994; Pinto da Costa et al., 1996; Caetano, 2000). In particular, the direct and parametric excitation of the cable in stayed-systems, investigated through an inclined cable model in Pinto da Costa et al. (1996), has evidenced that small amplitudes of the cable anchorage may cause significant cable oscillation when their frequency content is close to either one or two times the first natural frequency of the cable. The authors add to their conclusions that additional studies are needed to check the possible frequency range of the anchorage motion, particularly in long-span bridges where the risk of involving lower bridge modes in the interaction may be dangerous.

The present investigation aims to show that, besides the two mechanisms of excitation thus far presented in the literature, there is an unexplored source of cable vibration due to the nonlinear cable–beam interaction, induced by a global motion oscillating at half of the first cable frequency. This novel mechanism appears to have technical significance because it involves lower global modes which, being more flexible, are therefore prone to induce large anchorage motion. At the same time, the occurrence of global modes at lower frequency than local modes seems to be very common in recent constructions producing one-to-two global–local resonances in numerous situations (Abdel-Ghaffar and Khalifa, 1991; Brownjohn et al., 1999; Caetano et al., 2001; Au et al., 2001; Yamaguchi et al., 2001).

Aiming to explore this interaction mechanism, this paper presents a novel analytical model for a simple geometrically nonlinear cable coupled with an axially-rigid Euler–Bernoulli beam. The integro-partial differential equations, obtained using the Hamiltonian principle and the standard condensation procedure of the longitudinal cable displacement (Luongo et al., 1984), are able to describe the quadratic interaction at the cable–beam boundary and the cubic hardening behavior due to large transverse cable displacement. Hence, the homogeneous linearized equations are solved (Gattulli et al., 2002) and a parametric analysis

permits the determination of systems with a one-to-two ratio between the natural frequencies associated with local and global modes.

A 2dof discrete model, derived with the standard Galerkin method using the eigenfunction basis, has been used in the analysis involving only the resonant modes. This cable–structure interaction model permits the identification of the cable vibration sources and exploration of their relevance. Two different nonlinear phenomena due to quadratic coupling are evidenced through the analysis of the model response: *angle-variation* and *parametric* induced cable oscillations. The excitation mechanism due to the angle-variation of the cable tension during motion is newly presented and thoroughly discussed while peculiar aspects of the well-known parametrically induced cable oscillations are also pursued through the analytical model presented.

The paper is organized as follows. The governing relations of cable-stayed beam dynamics are presented through continuous and discrete models (Section 2). Results of eigenvalue sensitivity analyses conducted on the continuous linearized model are summarized (Section 3), particularly for the description of the one-to-two global–local resonant manifold (Section 3.1) and for the parameter influences on the occurrence of autoparametric two-to-one global–local resonance (Section 3.2). There follows a complete description of the effects of angle-variations in the cable tension on the nonlinear system dynamics (Section 4). First, the parameter sensitivity of relevant nonlinear interaction is discussed, then the dynamic response of systems in a perfect or internal detuned one-to-two global–local resonant condition is described (Section 4.1). The section concludes with a description of the chaotic dynamics emerging for a range of technically significant load amplitude and frequency values (Section 4.2). Next, local cable oscillations induced by autoparametric resonance are described through the model presented (Section 5). Concluding remarks summarize the research findings.

2. Cable-stayed beam model

The actual planar configuration of a cable-supported cantilever beam is described, with respect to the static equilibrium configuration, by the cable displacement components U_c, V_c and the beam transverse displacements V_b within the hypothesis extensively reported in Gattulli et al. (2002) (Fig. 1). Under the assumptions of small sag D to length L_c ratio (i.e. $D/L_c \leqslant \frac{1}{10}$), for the coordinate system shown in Fig. 1, the

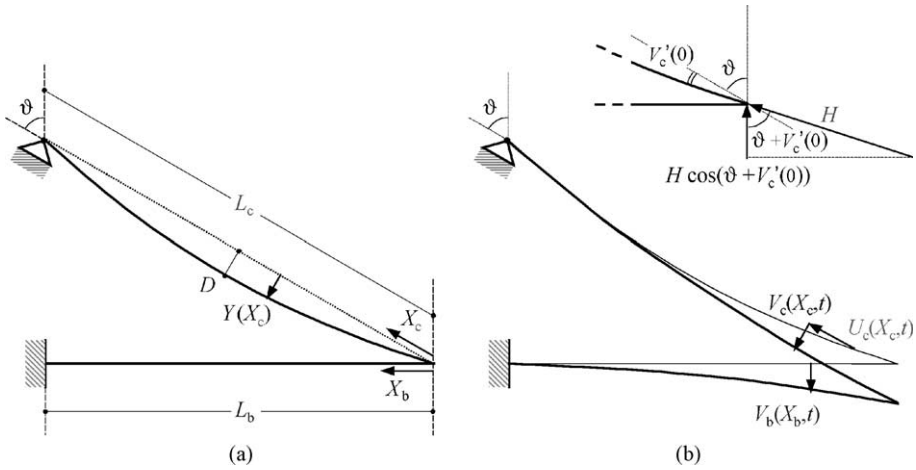

Fig. 1. Cable-stayed beam configurations: (a) reference, (b) actual.

equilibrium configuration for the inclined cable is described through the parabola $Y(X_c) = 4D[X_c/L_c - (X_c/L_c)^2]$. We denote ω_1 the first structural modal frequency; m_b and m_c the beam and cable mass density along the cable and beam length respectively; P_b and P_c the transverse loads; Ξ_b and Ξ_c the transverse damping density; E_bI_b the beam flexural stiffness; E_cA_c the axial stiffness; H the static cable tension. Neglecting the contribution of the longitudinal acceleration $\ddot{U}_c$ in the prevalent transverse cable motion, the axial, shear strain and the geometric nonlinearities of the beam, and defining the following non-dimensional quantities:

$$\begin{aligned} &y = \frac{Y}{D}; \quad \tau = \omega_1 t; \quad x_i = \frac{X_i}{L_i}; \quad v_i = \frac{V_i}{L_i}; \quad \xi_i = \frac{\Xi_i}{m_i\omega_1}; \quad p_i = \frac{P_i}{m_i L_i \omega_1^2} \qquad (i = b, c) \\ &\rho = \frac{m_c}{m_b}; \quad \mu = \frac{E_cA_c}{H}; \quad \nu = \frac{D}{L_c}; \quad \chi = \frac{E_bI_b}{L_b^2 E_cA_c}; \quad \beta_{b_1}^4 = \omega_1^2 \frac{m_b L_b^4}{E_bI_b}; \quad \beta_{c_1}^2 = \omega_1^2 \frac{m_c L_c^2}{H} \end{aligned} \tag{1}$$

by using the classical extended Hamilton's principle, the equations of motion governing the transverse vibration are obtained:

$$\begin{aligned} &\ddot{v}_b + \xi_b \dot{v}_b + \frac{1}{\beta_{b_1}^4} v_b'''' = p_b \\ &\ddot{v}_c + \xi_c \dot{v}_c - \frac{1}{\beta_{c_1}^2}\left[v_c' + \mu(\nu y' + v_c')\bar{e}\right]' = p_c \end{aligned} \tag{2}$$

where the functions v_b and v_c, for any value of τ, satisfy the following geometric boundary conditions:

$$\begin{aligned} &v_c(0) - v_b(0)\sin^2\vartheta = 0 \quad v_c(1) = 0 \\ &v_b(1) = 0 \qquad\qquad\qquad\quad v_b'(1) = 0 \end{aligned} \tag{3}$$

and the relevant mechanical boundary conditions at the beam tip,

$$\mu\chi v_b'''(0) - v_c'(0)\sin\vartheta = \mu[(\nu y'(0) + v_c'(0))\sin\vartheta - \cos\vartheta]\bar{e} \quad v_b''(0) = 0 \tag{4}$$

In Eqs. (2)–(4) apex and dot indicate differentiation with respect to the abscissa x and the non-dimensional time τ; and $\bar{e} = \bar{e}(\tau)$ represents the uniform dynamic elongation given by

$$\bar{e} = v_b(0)\sin\vartheta\cos\vartheta + \int_0^1 \left(\nu y' v_c' + \tfrac{1}{2}v_c'^2\right) dx_c \tag{5}$$

Eq. (2) with the boundary conditions expressed by Eqs. (3) and (4) describe the forced in-plane nonlinear oscillations of the cable-stayed beam. The equations governing the small amplitude structural oscillation can be obtained linearizing Eqs. (2)–(4) in the neighborhood of the equilibrium configuration.

An extensive analysis of the parameter sensitivity of the eigenproblem associated with Eqs. (2)–(5) is reported in Gattulli et al. (2002). These analyses have evidenced the existence of global and local modes (e.g. see Fig. 2).

In order to describe the nonlinear cable–beam interaction a Galerkin discretization of Eqs. (2)–(4) has been pursued, using a global and a local mode. In particular, the displacements have been expressed in the modal space as, $\mathbf{v} = \mathbf{\Phi q}$, where the displacement vector is ordered as $\mathbf{v} = \{v_b(x_b,\tau), v_c(x_c,\tau)\}^T$, the modal matrix $\mathbf{\Phi} = [\boldsymbol{\phi}_1 \,|\, \boldsymbol{\phi}_2]$ is composed by the eigenfunctions $\boldsymbol{\phi}_i = \{\phi_{bi}(x_b), \phi_{ci}(x_c)\}^T$ and the modal amplitude vector is $\mathbf{q} = \{q_1(\tau), q_2(\tau)\}^T$. Imposing the stationarity of the associated Hamiltonian, the following nonlinear ordinary differential equations are obtained:

$$\begin{aligned} &\ddot{q}_1 + \xi_1\dot{q}_1 + q_1 + c_{11}q_1^2 + c_{12}q_1q_2 + c_{22}q_2^2 + c_{111}q_1^3 + c_{112}q_1^2q_2 + c_{122}q_1q_2^2 + c_{222}q_2^3 = p_1 \\ &\ddot{q}_2 + \xi_2\dot{q}_2 + \omega_2^2 q_2 + d_{11}q_1^2 + d_{21}q_1q_2 + d_{22}q_2^2 + d_{111}q_1^3 + d_{211}q_1^2q_2 + d_{221}q_1q_2^2 + d_{222}q_2^3 = p_2 \end{aligned} \tag{6}$$

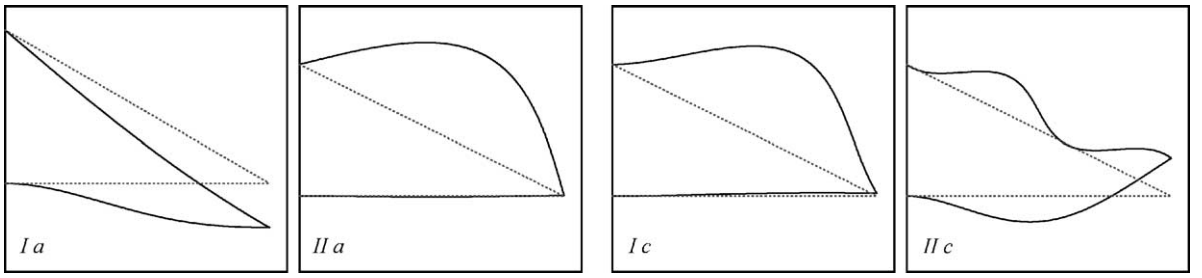

Fig. 2. Modal shapes of cable-stayed beam: system A (*Ia*—global mode, *IIa*—local mode); system C (*Ic*—local mode, *IIc*—global mode).

where c_{ij}, d_{ij}, c_{ijh} and d_{ijh} are the coefficients of complete quadratic and cubic polynomials, respectively. The polynomial coefficients and the amplitude of the modal loads, p_i, are reported in Appendix A. The system is forced by single-harmonic functions with non-dimensional frequency $\Omega = \omega/\omega_1$ used to span the frequency range where the nonlinear interaction is expected.

3. Internal resonant cable-stayed beam

Dynamic properties of a cable-stayed beam have evidenced the existence of global, local and hybrid modes (Gattulli et al., 2002). Here, the attention is focused on the nonlinear interactions between local and global modes; hence, the solution of the eigenproblem associated with the linearized equations (2)–(4) is used to individuate those systems that possess an integer ratio r between the natural frequencies, namely, the internal resonant cable-stayed beams. An analysis of the sensitivity to parameter variations has shown that a frequency associated with a local mode may move towards a global mode frequency, but when those frequencies become closer a veering happens. Analytical treatment of the problem and the related results are reported in Lepidi and Gattulli (2002).

Differently, the results of the analysis conducted for those systems having modes in a one-to-two resonant combination are here summarized. The occurrence of these resonances is crucial for the modal interaction when quadratic coupling characterizes the system. These internal resonances have been found possible in two cases: the global mode having a frequency twice or half that of the local one.

The dynamic effects related to the first case have been explored in literature through either single cable models, excited by a parametric longitudinal action at the boundary (Perkins, 1992; Lilien and Pinto da Costa, 1994; Pinto da Costa et al., 1996), or richer cable–beam models (Fujino et al., 1993). In the second case, the effect of external excitation at half of the first cable natural frequency due to superharmonic resonance has been evidenced in Lilien and Pinto da Costa (1994); however the cable–beam interaction has remained unexplored in cable-stayed structures, and it will prove to play a fundamental role in their dynamics. Therefore, in what follows, one-to-two resonant systems with a *global–local* modal sequence have been investigated. The analytical model has then also been used to evidence the parametric excitation of the cable by induced beam motion in a system with a one-to-two resonant *local–global* modal sequence.

In both previous cases, the response to external harmonic excitation of the global mode has been used to demonstrate the global–local interaction. Thus, the distances to the internal and external resonant conditions have been appropriately described through the relations

$$\omega_2 = 2\omega_1 + \sigma_1; \quad \Omega = \omega_1 + \sigma_2; \quad \Omega = \omega_2 + \sigma_3 \tag{7}$$

where σ_1 describes the internal detuning, while σ_2 and σ_3 are the detuning parameters of the forcing frequency at the primary resonance of the global mode, that is the first and the second mode respectively, in the two studied cases.

3.1. One-to-two global–local internal resonance

In order to individuate those systems with a one-to-two global–local sequence, an extensive analysis has been conducted on the sensitivity of the eigenvalues to the parameter variations. In particular, the analysis, differently from Gattulli et al. (2002), has been mainly devoted to describing the dependence of the eigenfrequency ratio r between the first and the second modes on the $(\rho, \chi, \vartheta, \mu)$-space. The involved modes have been classified as local, global and hybrid. The locus of points in the parameter space where $r = 0.5$ describes the one-to-two resonant manifold. The (ρ, χ, ϑ)-dependence of the ratio r is drawn in Fig. 3. The dependence of r versus the χ-parameter reflects the behavior of the system, where two limit cases, fixed-supported ($\chi \to 0$) and fixed-free beam ($\chi \to \infty$), have been recognized (Gattulli et al., 2002). For low values of χ, the first and the second modes are global (the cable is highly rigid); hence they converge to the ratio between the frequencies of the two first global modes of the fixed-supported beam ($r = 0.308$), no matter what mass ratio ρ and angle ϑ are considered. Increasing χ, the frequency of the second global mode decreases faster than the first global one, up to a certain value (the first relative maximum in Fig. 3a–c), where the influence of the third local mode becomes significant and produces a change on the rate of r versus χ. Still increasing χ, a veering between the frequencies of the second global and the first local (third for the system) modes is found and, as a direct consequence, a hybridization of their modal shapes appears. In this situation, the ratio r between the first and the second modes involves a global–hybrid sequence. Progressing along the χ-axis produces a flipping between the global and local modes involved in the veering. Finally, the systems with the searched global–local sequence in one-to-two resonant condition are found when the curves in Fig. 3 cross the bold straight line ($r = 1{:}2$). The described behavior can be followed for different ρ-values.

In Fig. 4a the ratio r is reported in the (χ, ϑ)-plane for a given ρ. On this plane, regions associated to different modal sequences are evidenced through different backgrounds, confirming that global–global, global–hybrid, global–local, hybrid–hybrid and hybrid–local sequences are possible for the first two modes in a cable-stayed beam.

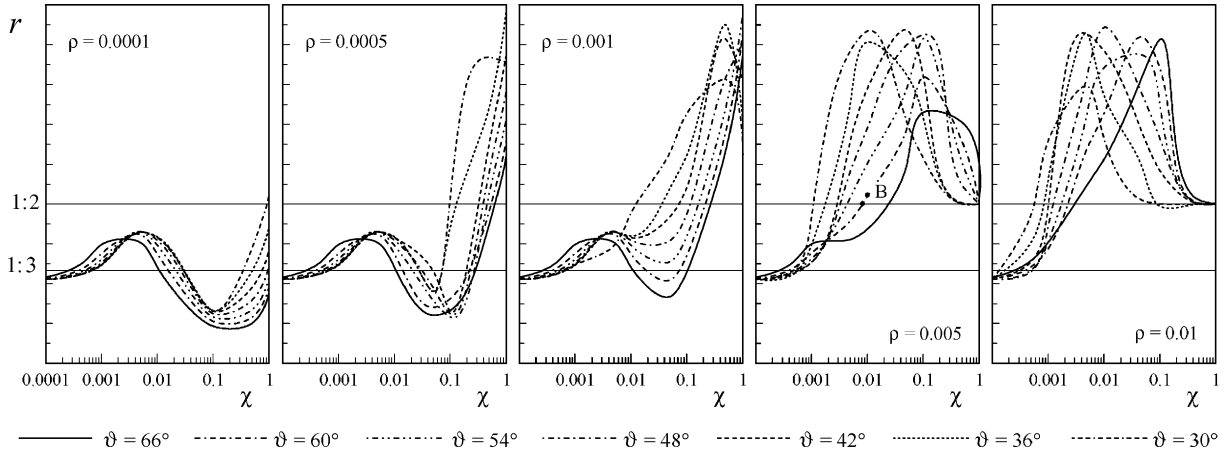

Fig. 3. (ρ, χ, ϑ)-dependence of the frequency ratio r between first and second eigenfrequencies.

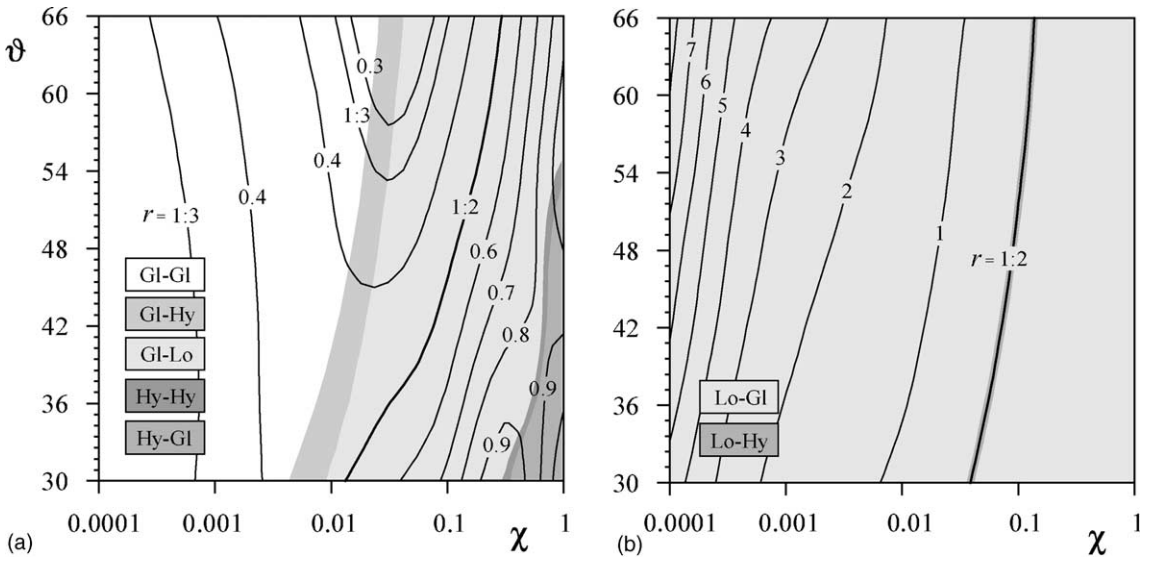

Fig. 4. Mode sequences and their frequency ratio r in the (χ, ϑ)-plane for $\rho = 0.001$: (a) first and second eigenfrequency ratio, (b) first local and second global eigenfrequency ratio.

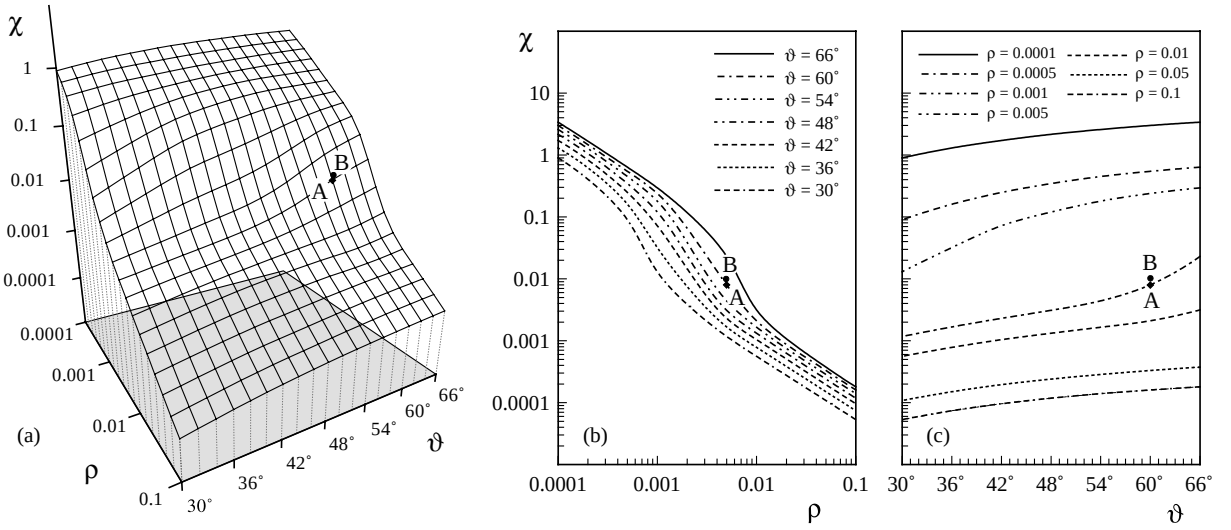

Fig. 5. One-to-two global–local resonant manifold ($\mu = 486$): (a) 3D view, (b) sections for different ϑ, (c) sections for different ρ.

The investigations evidence that a one-to-two resonance for a global–local sequence can be found within a range of values of technical interest. Therefore, the one-to-two resonant manifold can be described in the (ρ, ϑ, χ)-subspace for a given μ, as shown in Fig. 5. The 3D view (Fig. 5a) and the sections for different ϑ and ρ, respectively (Fig. 5b,c), show that the resonance is not very dependent on the angle between the cable and the beam while it occurs for (ρ, χ)-pairs having an almost constant ratio of the order of 10^4. An investigation into the influence of the μ-parameter, not reported for sake of brevity, shows that the shape of

the resonant manifold in the (ρ, ϑ, χ)-space remains unchanged, while the increase (decrease) of μ makes the manifold translate down (up) along the χ-axis.

3.2. Two-to-one global–local internal resonance

The research of two-to-one global–local resonant systems is more involved due to the difficulties of following the sensitivity to parameter variations of global mode with higher frequency. In this case, to get the searched sequence, the global mode must have a frequency higher than the local one; thus the modes having at least one node along the beam axis should be considered (mode type *IIc*, see Fig. 2d and Fujino et al., 1993; Gattulli et al., 2002). The research is also complicated by the occurrence of the one-to-two resonance between the first and the second local modes (perfectly resonant for a string, $\nu = 0$) (Pinto da Costa et al., 1996). Consequently, a system with a one-to-two local–global resonance has two close frequencies at twice the first local frequency: namely, the second local frequency (first asymmetric mode in the cable domain) and the second global frequency. Again, a very strict veering happens in this region.

A selection of results of these analysis are summarized in Fig. 4b where, for a given ρ, the ratio between a first-local and a second-global frequency is plotted in the (ϑ, χ)-plane. Resonant systems with local–global sequence are identified, and it is shown that a perfect two-to-one global–local ratio is disturbed by the hybridization of the global mode due to the veering with the second local one. Then we study the case of cable with sag ($\nu > 0$); the related augmentation of the ratio between the first and the second local frequencies makes possible the avoidance of systems with three modes involved in the resonance. However, in cases of technical interest for stayed-system, the sag is generally very small, then a modal distortion in the one-to-two local–global systems should generally be expected (Warnitchai et al., 1993; Pinto da Costa et al., 1996).

4. Interactions of one-to-two resonant global–local modes

A novel analysis has been performed to evidence the effects of an unexplored mechanism of cable excitation due to beam motion in stayed-systems. The studied model describes the mechanical cable–beam interaction at the tip by Eqs. (3) and (4), evidencing that the cable transverse motion is coupled with the beam tip displacement through the cable elongation, Eq. (5). The boundary interaction mechanism produces a quadratic coupling, which is due to the angle-variation between the cable tension and the beam axis during the motion. This mechanism, in the simple case $\nu = 0$, can be recognized in the shear-type boundary condition expressed by Eq. (4_1), such as

$$v_c'(0)\sin\vartheta(1+\mu\bar{e}) - \cos\vartheta\mu\bar{e} = \mu\chi v_b'''(0) \tag{8}$$

An easier interpretation of the mechanism could be made expressing Eq. (4) through the dimensional static, H, and dynamical, N, components of the cable tension and the shear T at the beam tip, see Fig. 1, yielding

$$(N+H)\cos(\vartheta + v_c'(0)) = T \tag{9}$$

The dynamic cable tension N is evaluated by the elongation as $N = H\mu\bar{e}$, $v_c'(0)$ is the angle between the actual and the reference configuration, and $T = E_b I_b v_b'''(0)$ is the shear at the beam tip. Eq. (9) shows that the boundary conditions express the equilibrium between the shear and the projection of the axial tension evaluated in the actual configuration of the cable, in accordance with the model assumptions. It should be noticed that Eq. (8) differs from Eq. (9) only for the approximation $\sin(v_c'(0)) \simeq v_c'(0)$ and for the presence of the static contribution $H\cos\vartheta$, which does not affect the dynamic equilibrium.

Substituting the expression of the cable elongation $\bar{e}$ in the boundary condition, the quadratic term $v_c'(0)v_b(0)\sin^2\vartheta\cos\vartheta$ arises. Its projection in the modal global–local basis, produces an internal quadratic

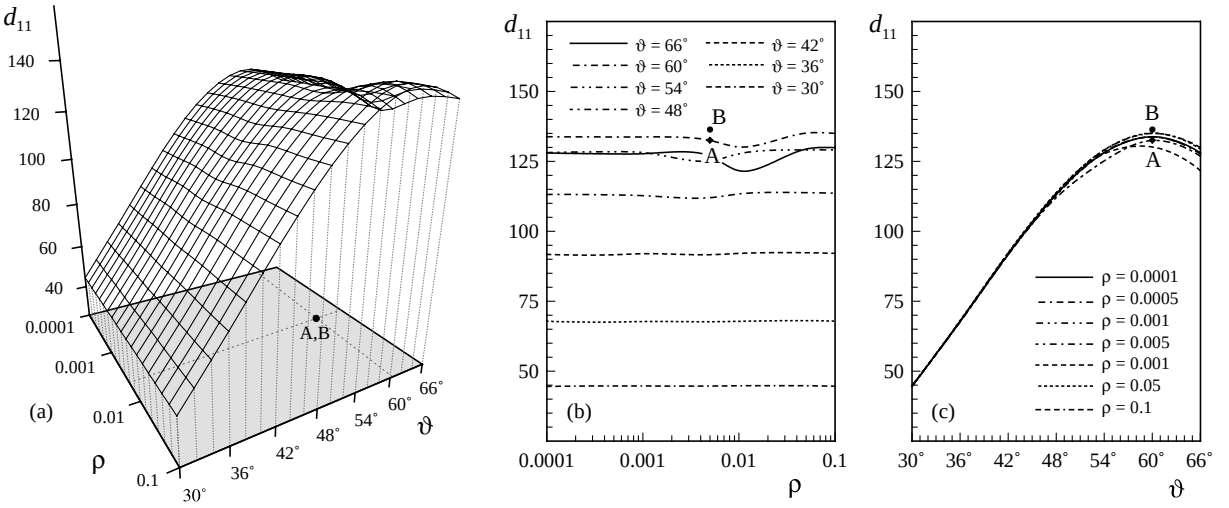

Fig. 6. Nonlinear coefficient d_{11} in the (ρ, ϑ)-plane: (a) 3D view, (b) sections for different ϑ, (c) sections for different ρ.

excitation of the cable represented by the term $d_{11}q_1^2$ in the local equation (6_2). Consequently, if the global motion, q_1, is directly excited at primary resonance $\Omega \simeq \omega_1$, the quadratic term $d_{11}q_1^2$ in Eq. (6_2) is able to excite the local motion at twice resonant frequency $2\omega_2 = \omega_1$ (superharmonic excitation; e.g. Haddow et al., 1984), producing large cable vibrations. The described modal interaction realizes a transfer of energy from low-global to high-local frequencies.

The quadratic excitation of the local mode, induced by global motion, represents a peculiarity of this mechanism different from the longitudinal *parametric* excitation (Lilien and Pinto da Costa, 1994), and from a direct excitation induced by an imposed transversal support motion (Pinto da Costa et al., 1996; Caetano, 2000).

To evidence the dynamical characteristics of this *angle-variation* interaction, a preliminary analysis has been conducted to select a candidate system. Hence, systems with a first global and a second local mode have been considered (see Fig. 2). As previously mentioned, the interest is on those cable-stayed beams belonging to the one-to-two resonant manifold depicted in Fig. 5. However, for these resonant systems, we have also investigated the sensitivity to the parameter variations of the coefficient d_{11}. The values assumed by d_{11} in the (ρ, ϑ)-plane are presented in Fig. 6, where the χ-dependence of the coefficient has been used to satisfy the resonant condition. The coefficient proves to be more sensitive to the ϑ-variation than to other parameter variations, confirming its strong dependence on the boundary condition term $v_c'(0)v_b(0)\sin^2\vartheta\cos\vartheta$ in Eq. (4), which assumes its maximum value around $\vartheta = 60°$.

The interaction is strongly influenced also by the term $d_{21}q_1q_2$ in the local equation (6_2), which derives from the discretization of the autoparametric term $v_c''v_b(0)\sin\vartheta\cos\vartheta$ (see Appendix A), obtained by substituting the cable elongation (Eq. (5)) in the cable equation (2_2). The parameter dependence of the coefficient d_{21}, depicted in Fig. 7, assumes its maximum value around $\vartheta = 45°$.

4.1. Cable oscillations induced by boundary angle-variation of the tension

The previous preliminary discussion has permitted selection of systems where a strong nonlinear modal interaction is expected. Two systems have been considered: the first one, A, in perfect one-to-two resonance, and the second one, B, detuned from it (see Table 1 and Figs. 4–7).

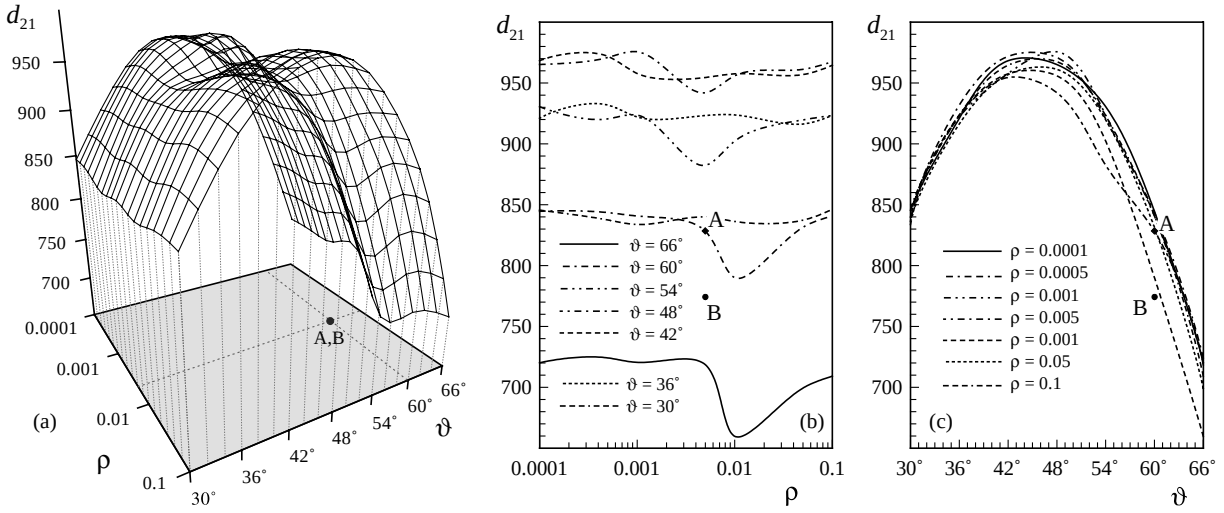

Fig. 7. Nonlinear coefficient d_{21} in the (ρ, ϑ)-plane: (a) 3D view, (b) sections for different ϑ, (c) sections for different ρ.

Table 1
Non-dimensional mechanical parameters of the selected cable-stayed beams

Pts	ρ	χ	ν	μ	ϑ	ξ_1	ξ_2	Modes	Description
A	0.005	0.008	0.0	486	60°	0.01	0.01	I, II	Global–local; 1:2 resonant
B	0.005	0.01	0.0	486	60°	0.01	0.01	I, II	Global–local; $\sigma_1 = -0.07$
C	0.01	0.03	0.022	486	60°	0.01	0.01	II, V	Local–global; 1:2 resonant
D	0.01	0.04	0.022	486	60°	0.01	0.01	II, V	Local–global; $\sigma_1 = 0.33$

The response of the system A, perfectly resonant, has been analyzed first. It exhibits the first global and the second local modes depicted in Fig. 3a,b.

The frequency response curves, named *frcs*, to an harmonic load applied to the global mode have been evaluated through the direct use of the pseudo-arclength continuation algorithm (Doedel and Kernevez, 1986) on the modal equations (6).

Fig. 8 shows the *frcs* to harmonic excitation of amplitude $p_1 = 0.0001$, $p_2 = 0.0$. The excitation of the global mode at the primary resonance yields a relevant coupling with the local mode due to the one-to-two internal resonance. In particular, at this excitation level, the frequency range involving the coupling phenomena, is spanned by the external detuning values, $\sigma_2 = \pm 0.05$; in this range, the energy exciting the global mode is transferred to the local mode.

The *frcs* of the global mode (Fig. 8a) and of the local mode (Fig. 8b) are multi-valued functions of the excitation frequency Ω. A technically relevant result is that, exciting the beam at certain given frequencies, the amplitudes of the local mode (q_2) are almost three times the amplitudes of the global one (q_1). Looking at the frequency dependence of the solutions, before the primary resonance for external detuning, $\sigma_2 < -0.04$, two stable periodic solutions co-exist, the first at small amplitude and the second with a similar level of local and global amplitudes. Moving the frequency towards the primary resonance, the local amplitude remains almost constant, while the global amplitude decreases to a certain frequency range, $-0.04 < \sigma_2 < -0.01$, where only one stable solution exists with large local mode amplitudes oscillating with a 2Ω frequency content.

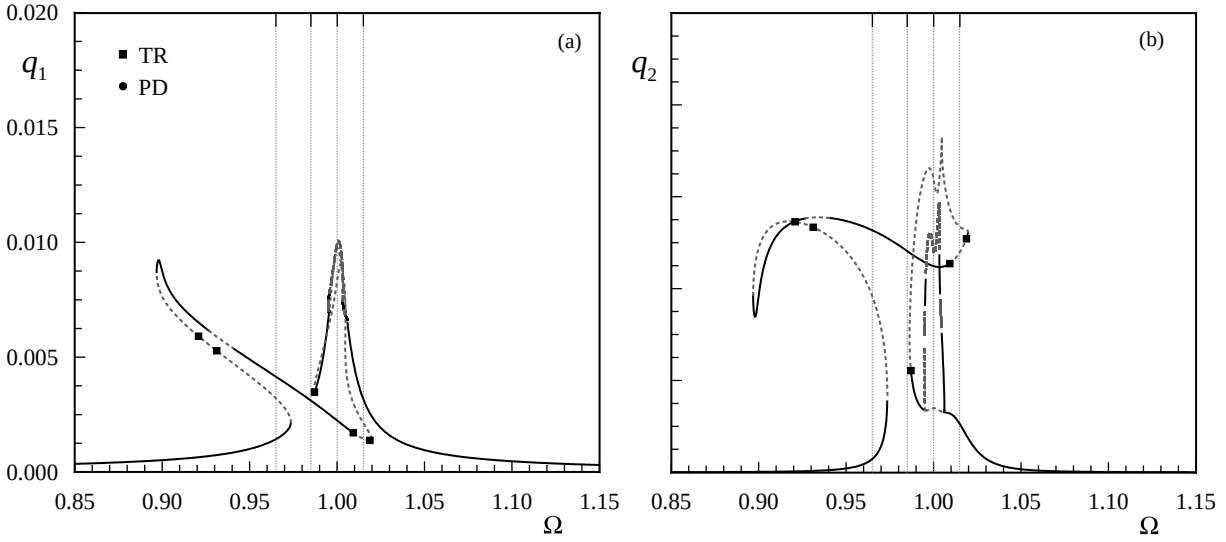

Fig. 8. Frequency response curves of modal amplitudes to global load $p_1 = 0.001$, for the system A in one-to-two internal resonance ($\sigma_1 = 0$): (a) global mode amplitude, (b) local mode amplitude.

When the external frequency is perfectly at the primary resonance of the global mode, $\sigma_2 = 0$, the *frc* of the global mode behaves almost linearly (see Fig. 8a). At this frequency resonance a loss of stability of the main branch through a period-doubling bifurcation is encountered similar to the ones occurring in Haddow et al. (1984) and Nayfeh and Balachandran (1990).

These *frcs* are quite different from the ones experienced, for examples, in the quadratic interactions at the primary resonance in Haddow et al. (1984), Nayfeh and Balachandran (1990) and Nayfeh (2001). The differences are due to the nature of the problems; indeed for cable-stayed beams the coefficients of the quadratic terms are larger in the local equation (6_2) than in the global one (6_1). Therefore, the symmetry of the *frcs* associated to perfectly resonant systems with similar modal masses is not confirmed for cable-stayed beams. Thus, the *frcs* of the cable-stayed beam systems show different amplitude levels in each of the two modes, with larger amplitudes in the local one. This is caused by the strong energy transfer to higher frequencies, which is strictly related to the particular mass ratio of the two sub-systems. This energy exchange also differs from the one occurring in the so-called *saturation* phenomenon, where the energy flows from high frequencies to low frequencies (Haddow et al., 1984; Nayfeh and Balachandran, 1990; Nayfeh, 2001).

Fig. 9 shows sections in the (p_1, Ω)-space of periodic solutions at different frequencies, for an increasing value of the load amplitude p_1. For frequencies smaller than the primary resonance (Fig. 9a,b), the amplitude of the local mode increases very fast with the augmentation of the load p_1 evidencing a relevant internal coupling. For large external detuning (Fig. 9a; $\sigma_2 = -0.035$) two co-existing stable solutions involve a larger portion of the load amplitude. Decreasing the external detuning (Fig. 9b; $\sigma_2 = -0.02$) the threshold of two co-existing stable solutions occurs at very low values for the load. Moving at the primary resonance, the behavior is complicated by the presence of a region of quasi-periodic and chaotic solutions described afterwards. At frequency higher than the primary resonance, increasing the excitation, the behavior is characterized by a jump from a branch of a single stable solution with similar local and global amplitudes to a branch of a single solution with higher local than global amplitude (Fig. 9c; $\sigma_2 = 0.015$).

In order to evaluate the effect of the internal detuning on the system response, a different system, B, has been considered (see Table 1). The system presents a natural frequency ratio of 1:1.93 which corresponds to

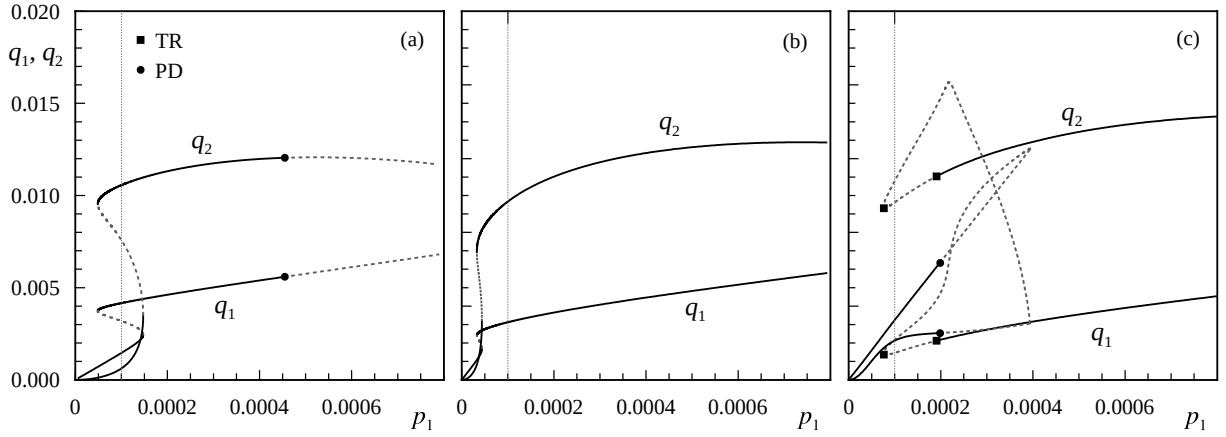

Fig. 9. Modal amplitudes for increasing load p_1 for the system A in one-to-two internal resonance ($\sigma_1 = 0$): (a) $\sigma_2 = -0.035$, (b) $\sigma_2 = -0.02$, (c) $\sigma_2 = 0.015$.

an internal detuning $\sigma_2 = -0.07$ and exhibits first global and second local mode similar to the ones depicted in Fig. 3a,b.

Fig. 10 shows the *frcs* to harmonic excitation exciting the global mode $p_1 = 0.0001$, $p_2 = 0.0$. The direct excitation of the global mode under primary resonance yields a resonant coupling with the local mode at the excitation frequency $2\Omega = \omega_2 = 1.93\omega_1 = 2(\Omega + \sigma_1)$ detuned with the primary resonance by the quantity $\sigma_1 = -0.035$.

Comparing the *frcs* of systems A and B, the effect of the detuning can be evaluated as a slight shift of the response. The detuning tightens the frequency range where only a single stable solution exists and it enlarges the range around the primary resonance where the solution is unstable.

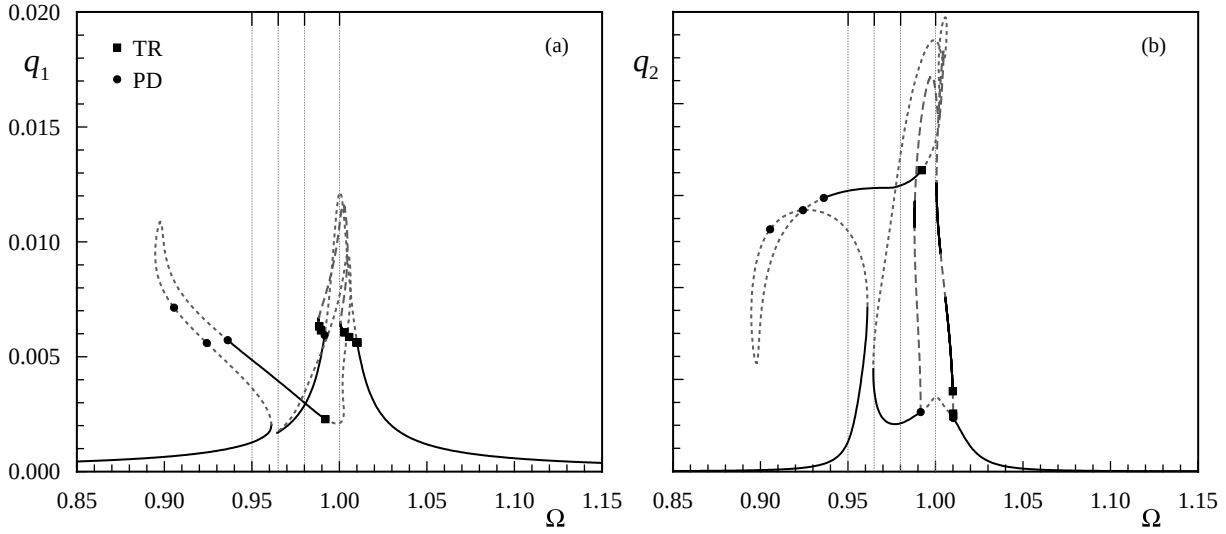

Fig. 10. Frequency response curves of modal amplitudes to global load $p_1 = 0.001$ for the system B detuned by the one-to-two internal resonance ($\sigma_1 = -0.07$): (a) global mode amplitude, (b) local mode amplitude.

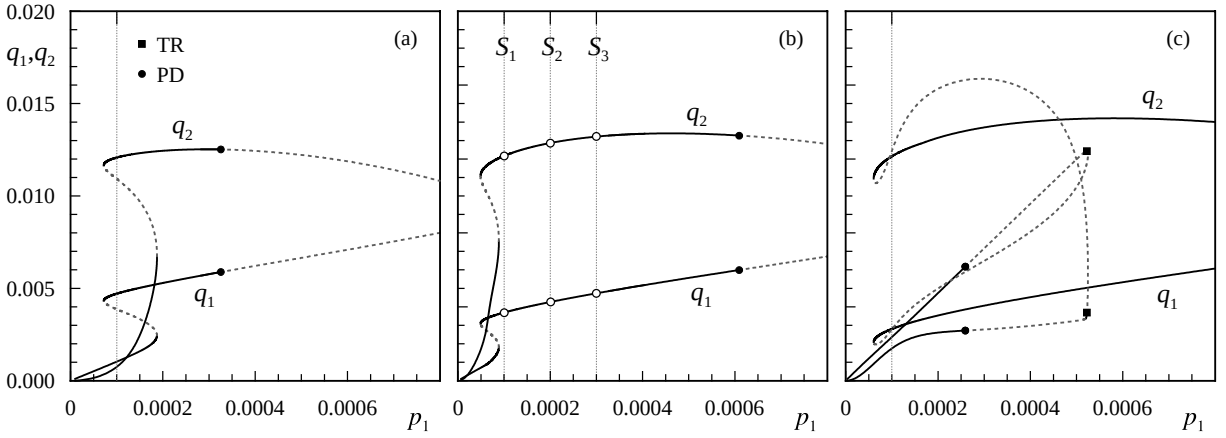

Fig. 11. Modal amplitudes for increasing load p_1 in the system B detuned by the resonance ($\sigma_1 = -0.07$): (a) $\sigma_2 = -0.05$, (b) $\sigma_2 = -0.035$, (c) $\sigma_2 = -0.02$.

Fig. 11 shows the sections in the (p_1, Ω)-space of periodic solutions at different excitation frequencies for system B. This case also confirms the immediate augmentation of the local amplitude up to values larger than the directly excited global one. The internal detuning is such that the larger portion of single periodic solutions occurs at the frequency $\Omega = 0.965$ that produces the quadratic term q_1^2 resonant with the local mode (Fig. 11b; $\sigma_2 = -0.035$). In this case, a periodic solution $S_1 = (0.0001, 0.965)$ in the (p_1, Ω)-space has been selected to quantify the frequency content of the two components; the results are presented in Fig. 12. Fig. 12a,b shows the transient response, starting at rest (i.e. $\mathbf{q} = \mathbf{0}$), where it is visible that the energy transfer needs time to be completed. Indeed while the global motion immediately reacts to the excitation with amplitudes smaller than at the steady state but significant, the local amplitudes grow almost linearly on a gradual slope. The frequency spectra of the steady-state solution (see Fig. 12c,d) have been calculated through a Fast Fourier Transform of the time histories (see Fig. 12a,b), showing a higher 2Ω component in the cable local motion, confirming the quadratic coupling mechanism. A detailed analysis of the energy transfer is omitted for sake of brevity and it will be presented in further publications.

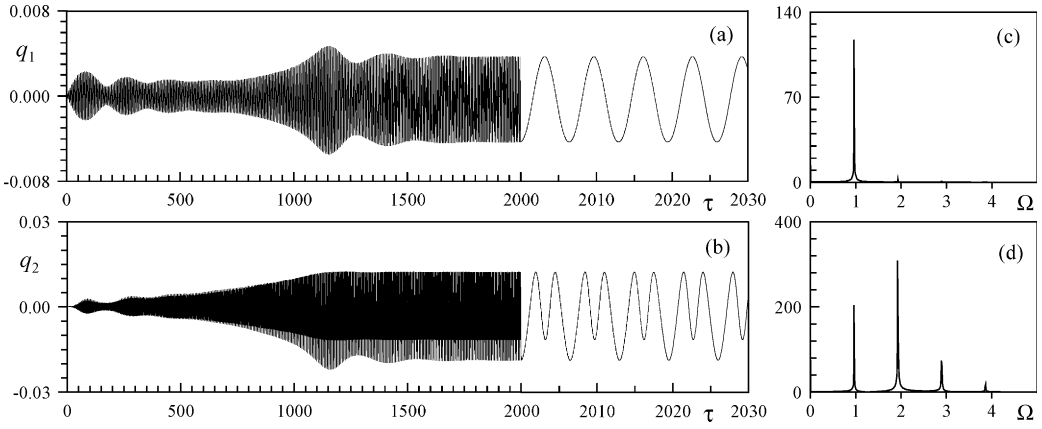

Fig. 12. Selected time histories of the periodic solution in the (p_1, Ω)-space; $S_1 = (0.001, 0.965)$; (a) and (b) global and local motion; (c) and (d) frequency spectra.

4.2. Chaotic response

The study of the periodic response of the one-to-two global–local resonant system has evidenced the mechanism of the interaction and the relevant oscillation amplitude reached by the local mode due to the energy transfer. However, looking at the *frcs*, the results clearly show that even for relatively low oscillation amplitudes of the global mode at the primary resonance, a response that never reaches a steady state can be observed. This region of unstable periodic solution, modified by the presence of an internal detuning, is present for both systems, A and B. A similar behavior of the *frcs* was first encountered in Haddow et al. (1984) and then deeply investigated in Nayfeh and Balachandran (1990) for a system with quadratic nonlinearities. In the latter case a transition from periodic oscillation to chaotic motion has been fully described.

Here, rather than completely describe the interesting transition from periodic to chaotic solutions, we have decided to point out only that such a scenario appears at a low level of global motion, if certain conditions are met with regard to the involved frequencies. In particular, we have made two sections of the *frcs* exactly at the primary resonance of the global mode, $\sigma_2 = 0.0$, for the systems A and B. In the case of the perfectly resonant system, A, the presence of a strong periodic attractor, for which large local periodic oscillations are admitted, is encountered up to a relatively large load amplitude, at which a period-doubling bifurcation occurs (see Fig. 13a). However, the occurrence of this bifurcation influences the scenario at lower levels of the load amplitude, where the second and higher unstable branches of solution appear, for which a cascade of successive period-doubling and torus bifurcations occur.

The presence of an internal detuning makes this scenario even more interesting, because the periodic attractor loses stability at very low load amplitude through a periodic-doubling bifurcation (see Fig. 13b). Following the second branch, which arises from the period-doubling bifurcation, a series of new period-doubling appears, opening frequency windows of unstable periodic and quasi-periodic solutions. Moving both the amplitude and the frequency of the external load, a series of periodic attractors have been found; for sake of brevity, just one example of this scenario is reported. Fig. 14 shows the main characteristics of a chaotic solution explored inside the (p_1, Ω)-space around the primary resonance of the global mode. The phase portraits of the solution are reported in Fig. 14a,b obtained in the time interval $4000 < \tau < 7000$.

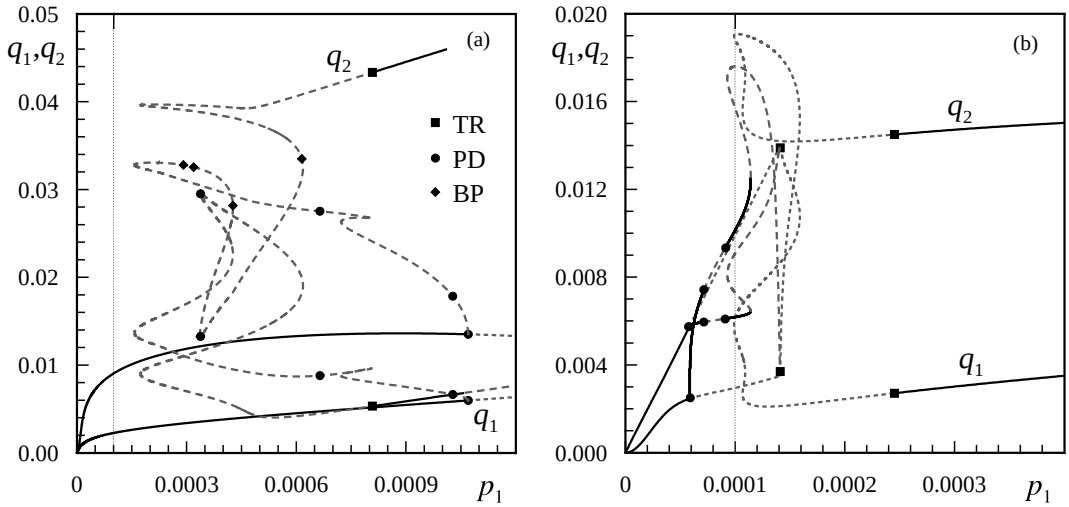

Fig. 13. Modal amplitudes for increasing load p_1 at the primary resonance: (a) system A ($\sigma_1 = 0.0$, $\sigma_2 = 0.0$); (b) system B ($\sigma_1 = -0.07$, $\sigma_2 = 0.0$).

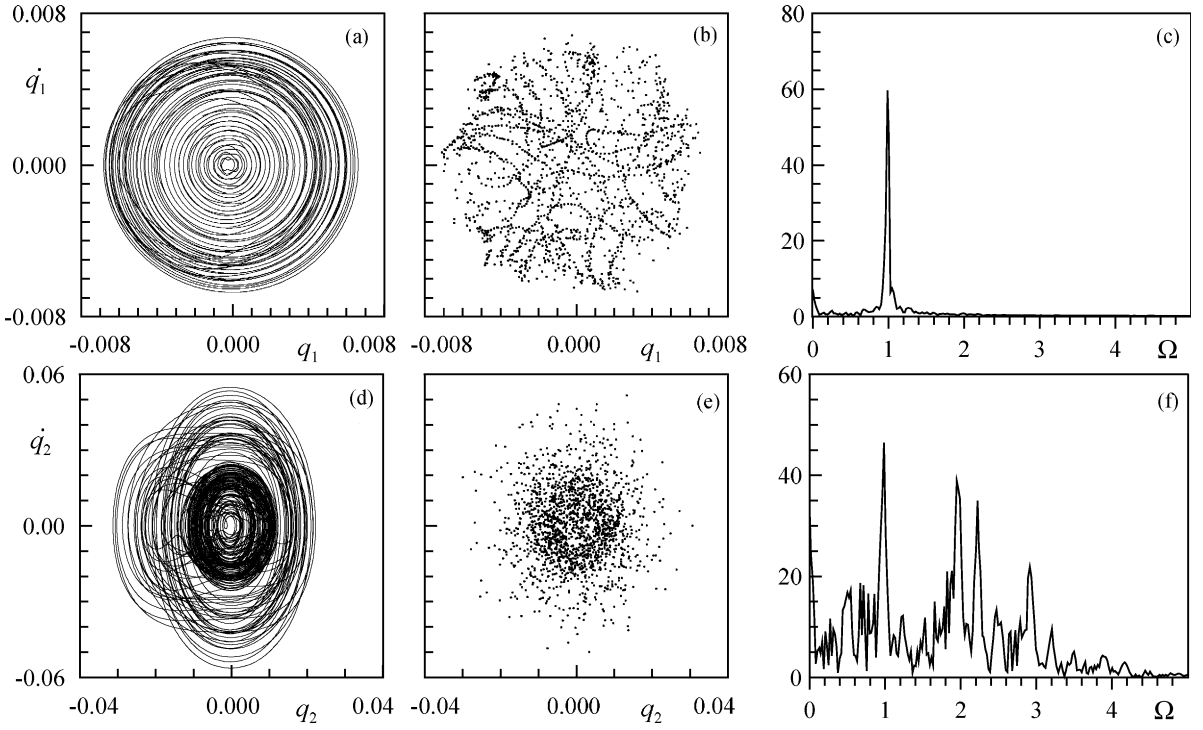

Fig. 14. Chaotic motion of the system B ($\sigma_1 = -0.07$, $\sigma_2 = 0.0025$): (a) and (b) phase portraits; (c) and (d) Poincaré sections; (e) and (f) frequency content of the global and local amplitudes.

In addition to the phase plots, the loss of periodicity of the solution can be characterized by Poincaré sections and frequency spectra, as has been depicted in Fig. 14c–f. However, more rigorous measures of the characteristics of various attractors or steady-state solutions can be pursued by Lyapunov exponents, and the various concepts of dimension associated with them. Here, following the procedure in Wolf et al. (1985), the first Lyapunov exponent λ, of the time series $q_1(\tau)$ and $q_2(\tau)$ depicted in Fig. 14, has been evaluated, confirming the complexity of the motion ($\lambda = 0.09$).

5. Interactions of two-to-one global–local modes

The second mechanism of cable excitation is related to the longitudinal imposed motion at the end of the cable, known as cable parametric excitation (Perkins, 1992; Fujino et al., 1993; Lilien and Pinto da Costa, 1994; Pinto da Costa et al., 1996; Caetano, 2000), more recently used as a control action (Warnitchai et al., 1993; Achkire and Preumont, 1996; Gattulli et al., 1997; Magaña and Rodellar, 1998). This interaction between the cable and the beam is described through a 2dof autoparametric discrete system selected by the model of Eqs. (2)–(4); indeed, as previously described, considering the cable elongation in Eq. (5), the quadratic term $v_c'' v_b(0) \sin\vartheta \cos\vartheta$ can be identified in the equation of the cable domain, Eq. (2_2). The quadratic expression projected on a selected local–global basis produces a term $q_1 q_2$ in Eq. (6_1) representing in this case the selected local modes. Thus, when the forcing global mode, q_2, has a frequency twice of the local mode, it produces a large oscillation described by a Mathieu-equation, typical of cable parametric excitation (Perkins, 1992; Lilien and Pinto da Costa, 1994).

5.1. Cable oscillations induced by boundary parametric longitudinal motion

The parametric excitation of the cable is here investigated through the cable-stayed beam model. A system with a global mode having a natural frequency twice that of a local one has been selected (system C, in Table 1). The modes involved in the nonlinear interaction are a first-type local and a second-type global modes (respectively, second and fifth modes for the coupled system, see also Table 1) with frequency ratio 1:2.05, represented in Fig. 2c,d. For this interaction, the discrete model is described by Eq. (6) where q_1 and q_2 represent, respectively, the local and global modal amplitudes. Eq. (6) present quadratic and cubic complete polynomials where the term $v_c'' v_b(0) \sin\vartheta \cos\vartheta$, responsible of the autoparametric excitation of the cable, produces mainly the quadratic term $c_{12} q_1 q_2$ in Eq. (6_1). Fig. 15 shows the *frcs* to harmonic excitation with modal amplitude forces $p_1 = 0.0$, $p_2 = 0.0001$. A relevant local mode response is obtained through the excitation of the global mode at its own primary resonance. In particular, if the forcing frequency is $\Omega \simeq 2.0$ the term $c_{12} q_1 q_2$ of Eq. (6_1) gets a frequency content $\Omega - \omega_1 \simeq 1.0 = \omega_1$ in resonance with the local mode, realizing its autoparametric excitation.

Different from the previous case, large cable oscillations appear suddenly after the bifurcation value of q_1, at which a period-doubling occurs. The locus of the points, PP′Q′Q where the period-doubling bifurcations happen is projected on the frequency–amplitude plane as shown in Fig. 15b. This locus is mainly dependent on the internal detuning and on the damping coefficients of the two oscillators. In particular, the minimum amplitude at which the bifurcation occurs corresponds with a frequency double of the local mode ($\Omega = 2\omega_1 + \sigma$ with $\sigma = \sigma_1 + \sigma_3 = 0$). The *frcs* presented in Fig. 15 has an asymmetric behavior induced by a small internal detuning, but, differently from the cases presented in Haddow et al. (1984) and Nayfeh and Balachandran (1990), higher amplitudes occur at higher frequency, because of the strong hardening behavior induced by cubic nonlinearities in the local mode. The system presents the *saturation* phenomenon in that, increasing the external loading after the bifurcation, the autoparametrically excited local amplitude increases faster than the directly forced global amplitude, which saturates. Here, the presence of cubic nonlinearities produces a slight augmentation of the global amplitude after the bifurcation (see Fig. 16), as has been shown in Gattulli et al. (1997). The critical bifurcation load amplitude p_2 for which local oscil-

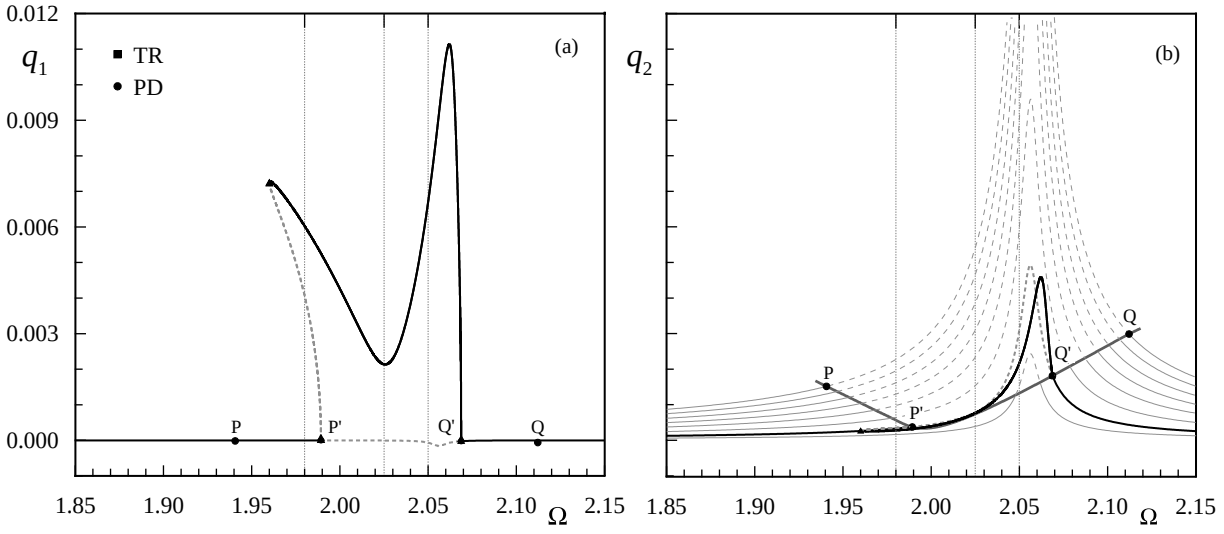

Fig. 15. Frequency response curves of modal amplitude to global load $p_2 = 0.001$ for the system C lightly detuned from two-to-one internal resonance ($\sigma_1 = 0.05$): (a) global mode amplitude, (b) local mode amplitude, PP′Q′Q period-doubling locus.

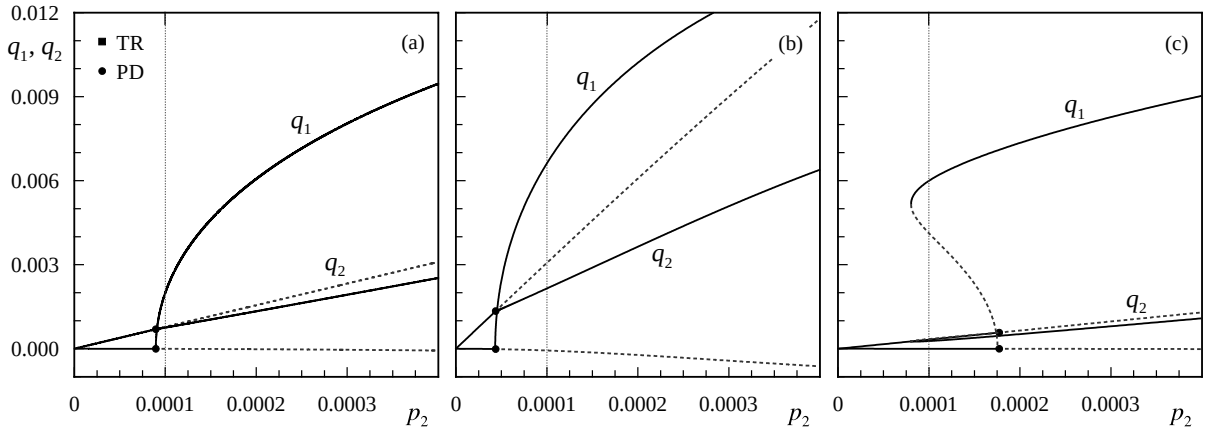

Fig. 16. Modal amplitudes for increasing load p_2 in the system C lightly detuned from two-to-one internal resonance ($\sigma_1 = 0.05$): (a) $\sigma_3 = -0.07$, (b) $\sigma_3 = -0.025$, (c) $\sigma_3 = 0.0$.

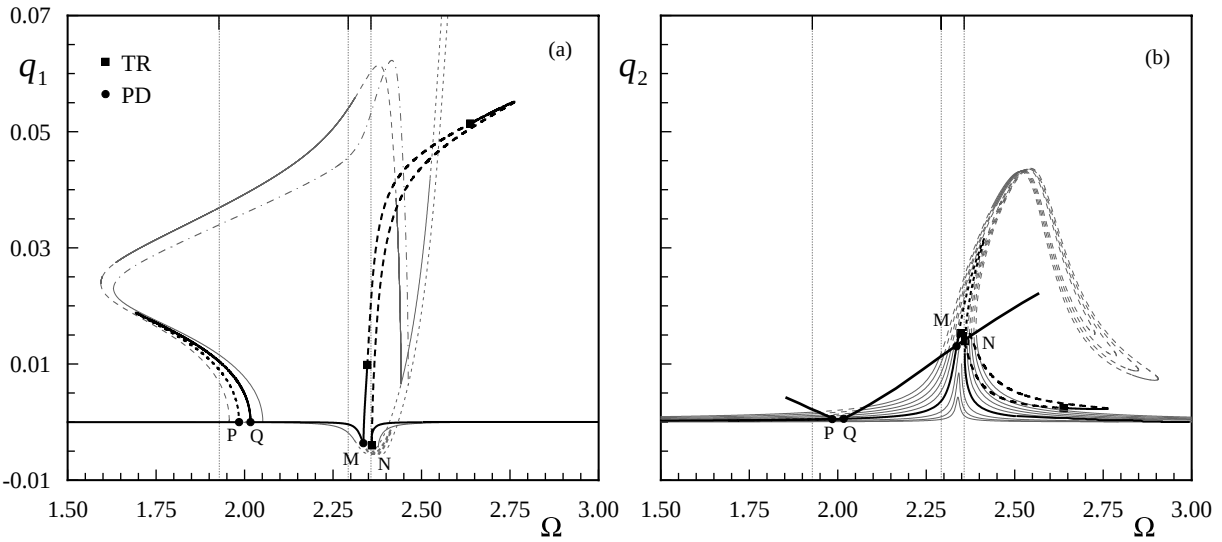

Fig. 17. Frequency response curves of modal amplitudes to global load $p_2 = 0.0008$ (bold lines) and $p_2 = 0.002$ (light lines) for the system D strongly detuned from two-to-one internal resonance system ($\sigma_1 = 0.34$): (a) global mode amplitude, (b) local mode amplitude; PQMN period-doubling locus.

lation appears depends directly on the detuning σ with respect to the autoparametric condition (see Fig. 16a–c).

Increasing substantially the internal detuning, as in the case of system D in Table 1, produces a weaker interaction between the primary resonance and the autoparametric resonance due to the frequency distance. Consequently, the autoparametric resonance mechanism starts at a frequency close to double of the local frequency (around $\Omega = 2$), at the same level of global motion as the previous case, which is reached with a larger load amplitude p_2. The two mechanisms of resonance, primary and autoparametric, do not interact with each other up to a certain load amplitude where a period-doubling bifurcation occurs. The two

branches of bifurcated solutions are clearly depicted in Fig. 17 for different levels of excitation, where at low excitation level (bold lines) large local vibrations may occur at both the autoparametric and the primary resonances (Fig. 17a). Both bifurcated branches are due to the autoparametric mechanism that, at this level of excitation, possess a global motion amplitude inside the Mathieu-region, which boundary is described by the locus of the bifurcation points PQMN, both at the autoparametric and at the primary resonances (see Fig. 17b). Increasing the load, an interaction between the two bifurcated branches occurs because the branch arising in the autoparametric frequency region ($\Omega \simeq 2$) bends towards higher frequency (see light curves in Fig. 17).

6. Concluding remarks

A correct modeling of cable–beam interaction proves relevant to describing the dynamic response of stayed-structures. Many phenomena associated with large cable vibrations have been investigated for their direct consequence on the dynamics of structures such as cable-stayed bridges, guyed-masts and suspended roofs. Some of these phenomena have been studied under a variety of models in the technical literature, others remain unexplored.

The present paper, through a newly developed analytical model of cable–beam interaction, evidences the effects of two internal resonant mechanisms which are potential causes of large cable oscillations.

The angle-variation mechanism seems to be a newly identified source of potential cable oscillations induced by beam motion. The inherent quadratic interaction of the mechanism is fully explained through the analytical model presented. Its effects appear to be more relevant in the presence of one-to-two global–local resonances, where the nonlinearities produce a transfer of energy from low to high frequencies and consequently large cable vibrations. An extensive discussion of the sensitivity of this resonance to the parameter variations has been presented based on the analytical treatment of the eigenvalue problem. The analysis has permitted us to determine the one-to-two resonant manifold in the parameter–space; further investigations have evidenced a class of resonant systems for which the largest interactions are expected. To describe the characteristics of the involved dynamics, different 2dof discrete systems composed of a global and a local mode, namely A and B, have been considered; the first one representing a perfectly resonant system and the second one used to evaluate the effects of an internal detuning. The *frcs* to harmonic loading of the global mode have been used to describe the role of the interaction in the dynamic response. Stable periodic solutions with a large local amplitude have been found in both systems. For some selected cases, the superharmonic energy transfer from low-*global* to high-*local* frequencies has been evaluated and explained. In a certain range of frequency, for relatively low global amplitudes, chaotic motions have been found. A very preliminary analysis of the chaotic dynamics has been pursued, evaluating the first Lyapunov exponent for a selected time series.

The autoparametric excitation mechanism of cables, contained in the developed analytical model, has been investigated especially with respect to the internal detuning sensitivity. Most of the results presented by Fujino et al. (1993) have been recovered in the present analysis. However, the present analysis offers a more precise description of the modes involved in the two-to-one global–local resonance. The effects of the internal detuning have been considered through the use of two different systems, namely C and D. The response analysis is pursued through the *frcs* to harmonic excitation on the global mode, around its primary resonance. For a certain level of global amplitude a period-doubling bifurcation occurs that produces relevant local amplitudes through a subharmonic autoparametric mechanism. This is accompanied by the well-known saturation phenomenon that here, however, shows some peculiarities due to the presence of cubic nonlinearities retained in the presented analyses. Finally, the effects of a strong positive internal detuning have been considered, evidencing that internal detuning augments the load value at which the autoparametric mechanism starts; but, surpassing this level, strong interaction between the autoparametric

and primary resonant branches occurs, producing an overall enlargement of the frequency region where large cable oscillations may be produced.

The description of both interaction mechanisms emphasizes the different nature of the physical phenomena. However, it permits a direct comparison of their effects on the dynamic response of cable-stayed structures, especially with respect to the main concerns regarding induced cable oscillations. Experimental validation of the angle-variation mechanism in the beam–cable interaction and characterization of the chaotic motions experienced at technically relevant values of the parameters have been already pursued; the results are under the current attention of the authors for possible future publication.

Acknowledgement

This work was partially supported by MURST (COFIN 01-02).

Appendix A

The coefficients of the quadratic and cubic terms of Eq. (6) are defined as

$$\begin{aligned} c_{ij}^{k} &= \frac{\mu}{m_k}\left\{\cos\vartheta\sin\vartheta\left[\phi_{\mathrm{b}_j}(0)I_{ki}^{e_\mathrm{c}}+\frac{2\phi_{\mathrm{b}_k}(0)I_{ij}^{e_\mathrm{c}}}{1+3\delta_{ij}}\right]+\nu\left[I_{ki}^{e_\mathrm{c}}I_{i}^{y}+\frac{2I_{k}^{y}I_{ij}^{e_\mathrm{c}}}{1+3\delta_{ij}}\right]\right\} \\ c_{ijh}^{k} &= \frac{\mu}{m_k}\left[(1-\delta_{ij})I_{kj}^{e_\mathrm{c}}I_{ih}^{e_\mathrm{c}}+\frac{1}{2}I_{ki}^{e_\mathrm{c}}I_{jh}^{e_\mathrm{c}}\right]\quad k=1,2 \end{aligned} \tag{A.1}$$

where δ_{ij} is the Kronecker symbol. Note that in Eq. (6) the following symbolic relations have been used to simplify the expressions: $c_{ij}^{1}=c_{ij}$, $c_{ij}^{2}=d_{ij}$, $c_{ijj}^{1}=c_{ijj}$, $c_{ijh}^{2}=d_{ijh}$. The following integrals have been used in Eq. (A.1):

$$\begin{aligned} &I_{i}^{y}=\int_0^1 y'\phi'_{\mathrm{c}_i}\,\mathrm{d}x\quad I_{ij}^{e_\mathrm{c}}=\int_0^1\phi'_{\mathrm{c}_i}\phi'_{\mathrm{c}_j}\,\mathrm{d}x\quad I_{ij}^{e_\mathrm{b}}=\int_0^1\phi''_{\mathrm{b}_i}\phi''_{\mathrm{b}_j}\,\mathrm{d}x \\ &I_{ij}^{m_\mathrm{c}}=\int_0^1\phi_{\mathrm{c}_i}\phi_{\mathrm{c}_j}\,\mathrm{d}x\quad I_{ij}^{m_\mathrm{b}}=\int_0^1\phi_{\mathrm{b}_i}\phi_{\mathrm{b}_j}\,\mathrm{d}x\quad I_{i}^{p}=\int_0^1(\phi_{\mathrm{c}_i}p_\mathrm{c}+\phi_{\mathrm{b}_i}p_\mathrm{b})\,\mathrm{d}x \end{aligned} \tag{A.2}$$

where ϕ_{c_i} and ϕ_{b_i} are the components of the selected mode, while p_c and p_b are the spatial distributions of the loads. The discrete quantities related to the mass, damping and excitation should be also introduced:

$$m_k=\beta_{\mathrm{c}_1}^2\left(I_{kk}^{m_\mathrm{c}}+\frac{1}{\rho}\sin^3\vartheta I_{kk}^{m_\mathrm{b}}\right);\quad \xi_k=\frac{\beta_{\mathrm{c}_1}^2}{m_k}\left(\xi_\mathrm{c}I_{kk}^{m_\mathrm{c}}+\frac{\xi_\mathrm{b}}{\rho}\sin^3\vartheta I_{kk}^{m_\mathrm{b}}\right);\quad p_k=\frac{I_k^p}{m_k} \tag{A.3}$$

where the coefficients ξ_k are related with the more common modal damping ratio $\hat{\xi}_k$ through the relation $\xi_k=2\omega_k/\omega_1\hat{\xi}_k$.

References

Abdel-Ghaffar, A.M., Khalifa, M.A., 1991. Importance of cable vibration in dynamics of cable-stayed beam. ASCE, J. Engng. Mech. 117 (11), 2571–2589.

Achkire, Y., Preumont, A., 1996. Active tendon control of cable-stayed bridges. Earthquake Engng. and Structural Dynamics 25 (6), 585–597.

Au, F.T.K., Cheng, Y.S., Cheung, Y.K., Zheng, D.Y., 2001. On the determination of natural frequencies and mode shapes of cable-stayed bridges. Appl. Mathematical Modelling 25, 1099–1115.

Barsotti, R., Ligaró, S.S., Royer-Carfagni, G.F., 2001. The web bridge. Int. J. Solids and Structures 38, 8831–8850.

Brownjohn, J.M.W., Lee, J., Cheong, B., 1999. Dynamic performance of a curved cable-stayed bridge. Engng. Structures 21, 1015–1027.

Caetano, E., 2000. Dynamics of cable-stayed bridges: experimental assesment of cable–structure interaction. Ph.D. Thesis, Porto.

Caetano, E., Cunha, A., Taylor, C.A., 2001. Investigation of dynamic cable–deck interaction in a physical model of a cable-stayed bridge: Part I. Modal analysis; Part II. Seismic response. Earthquake Engng. and Structural Dynamics 29, 499–521.

Casas, J.R., 1995. Full scale dynamic testing of the Alamillo cable-stayed bridge in Sevilla (Spain). Earthquake Engng. and Structural Dynamics 24 (1), 35–51.

Doedel, E., Kernevez, J.P., 1986. AUTO:Software for continuation and bifurcations problem in ordinary differential equations. Applied Mathematics Report, California Institute of Technology.

Fujino, Y., Warnitchai, P., Pacheco, B.M., 1993. An experimental and analytical study of autoparametric resonance in a 3DOF model of cable-stayed-beam. Nonlinear Dynamics 4, 111–138.

Gattulli, V., Morandini, M., Paolone, A., 2002. A parametric analytical model for nonlinear dynamics in cable-stayed beam. Earthquake Engng. and Structural Dynamics 31, 1281–1300.

Gattulli, V., Paolone, A., 1997. Planar motion of a cable-supported beam with feedback controlled actions. J. Intelligent Material and Structures 8 (9), 767–774.

Gattulli, V., Pasca, M., Vestroni, F., 1997. Nonlinear oscillations of a nonresonant cable under in-plane excitation with a longitudinal control. Nonlinear Dynamics 14, 139–156.

Gentile, C., Martinez Y Cabrera, F., 1997. Dynamic investigation of a repaired cable-stayed bridge. Earthquake Engng. and Structural Dynamics 26, 41–59.

Haddow, A.G., Barr, A.D.S., Mook, D.T., 1984. Theoretical and experimental study of modal interaction in a two-degree-of-freedom structure. J. Sound and Vibration 97 (3), 451–473.

Lepidi, M., Gattulli, V., 2002. Curve veering and crossing in selected eigenvalues problems. Internal Report DISAT, University of L'Aquila.

Lilien, J.L., Pinto da Costa, A., 1994. Vibration amplitudes caused by parametric excitations of cable stayed structures. J. Sound and Vibration 174, 69–90.

Luongo, A., Rega, G., Vestroni, F., 1984. Planar nonlinear free vibrations of elastic cable. Int. J. Non-linear Mech. 19, 39–52.

Magaña, M.E., Rodellar, J., 1998. Nonlinear decentralized active tendon control of cable-stayed bridges. J. Structural Control 5 (1), 45–62.

Nayfeh, A.H., 2001. Nonlinear interactions: analytical, computational, and experimental methods. John Wiley.

Nayfeh, A.H., Balachandran, B., 1990. Experimental investigation of resonantly forced oscillations of a two-degree-of-freedom structure. Int. J. Non-linear Mech. 25, 199–209.

Nazmy, A.S., Abdel-Ghaffar, A.M., 1990. Nonlinear earthquake-response analysis of long-span cable-stayed bridges: Part I. Theory; Part II. Applications. Earthquake Engng. and Structural Dynamics 19, 45–62, 63–76.

Perkins, N.C., 1992. Modal interactions in the non-linear response of elastic cables under parametric/external excitation. Int. J. Non-Linear Mech. 27, 233–250.

Pinto da Costa, A., Martins, J.A.C., Branco, F., Lilien, J.L., 1996. Oscillations of bridge stay cables induced by periodic motions of deck and/or towers. ASCE, J. Engng. Mech. 122 (7), 613–622.

Yamaguchi, H., Nishimura, T., Tsutsumi, K., Yamaguchi, K., 2001. Damping effect of coupled cable vibration in a cable-stayed bridge. In: Fourth Symposium on Cable Dynamics, Montreal, CA, pp. 153–160.

Warnitchai, P., Fujino, Y., Pacheco, B.M., Agret, R., 1993. An experimental study on active tendon control of cable-stayed bridges. Earthquake Engng. and Structural Dynamics 22, 93–111.

Warnitchai, P., Fujino, Y., Susumpow, T., 1995. A non-linear dynamic model for cables and its application to a cable–structure system. J. Sound and Vibration 187 (4), 695–712.

Wolf, A., Swift, J.B., Swinney, H.L., Vastano, J.A., 1985. Determining Lyapunov exponents from a time series. Physica D 16, 285–317.